

Passive cavitation imaging using an open ultrasonic system and time reversal reconstruction

P. Boulos^{a,b}, F. Varray^a, A. Poizat^{a,b}, J.C. Bera^b, C.Cachard^a

a. Université de Lyon, Creatis ;CNRS UMR5220 ; Inserm U1044 ; INSA-Lyon ; Université Claude Bernard Lyon 1, France

b.Université de Lyon, Inserm U1032,LabTau; Université Claude Bernard Lyon 1, France

Résumé :

Les maladies cardiovasculaires sont la première cause de mortalité dans le monde. Elles sont le plus souvent provoquées par l'obstruction des vaisseaux par des caillots sanguins entraînant un manque d'oxygène dans les cellules. La thrombolyse ultrasonore extracorporelle constituerait un traitement innovant utilisant des ultrasons focalisés pour détruire les caillots sanguins en tirant parti de l'aspect mécanique de la cavitation acoustique. Un prototype a été conçu afin de contrôler l'activité de cavitation. Pour suivre le processus de cavitation en temps réel, un système d'imagerie ultrasonore ouvert est en cours de développement. Les données brutes sont acquises en utilisant une sonde linéaire de 64 éléments actifs dans un mode d'imagerie passive. Lors du traitement de ces données, sur le principe du retournement temporel, le signal acoustique enregistré par la sonde est retro-propagé afin de localiser l'activité de cavitation.

Abstract:

Cardiovascular diseases are the first cause of mortality in the world. They are mostly caused by blood clots obstructing vessels which lead to a lack of oxygen in the cells. Extracorporeal ultrasound thrombolysis could be an innovative treatment using high intensity focused ultrasound to destroy blood clots by exploiting the mechanical aspect of the acoustic cavitation. A prototype has been designed and improved in order to control the cavitation intensity. To monitor the treatment in real time, an open ultrasound imaging system has been incorporated. Raw data have been acquired using a linear probe of 64 active elements in a passive imaging mode. Using the time reversal method, acoustic signal recorded by the probe is back propagated in order to estimate the location of the cavitation activity.

Keywords:ultrasound;thrombolysis; acoustic cavitation;monitoring;time reversal

1 Introduction

Ultrasound (US) imaging is mostly used for diagnostic imaging thanks to its known advantages as noninvasive, ease of use, real time display and cheap. However US can also be used for therapeutic treatments as for example high intensity focused ultrasound (HIFU) for tissue ablation [1], lithotripsy using US shock waves for the destruction of kidney stones [2] or US thrombolysis used for the destruction of blood clots [3].

Thrombolysis consists in destroying chemically and/or mechanically blood clots obstructing the vessels. Currently many thrombolysis techniques are used: surgeries (bypass or balloon angioplasty), and drug treatment using thrombolytic agents as tissue plasminogen activator (tPA), in which ultrasound sonoporation could be used to enhance the permeability of cell membrane relative to thrombolytic agent [4]. Yet these techniques have high risk of failure caused almost entirely by bleedings. Focused US induces in the medium acoustic cavitation which is related to bubbles created by a high acoustic depression. These bubbles can be seen in two phases. First, for low pressure non-inertial cavitation, also called boiling or stable cavitation, occurs when bubbles radially oscillate and induce thermal damages. Second, for higher pressure, inertial cavitation can appear which consists in bubble collapses generating shock waves with mechanical damages. US thrombolysis mainly uses the inertial cavitation for inducing mechanical damages on the blood clots. This inertial cavitation is very complex and unstable and research are conducted on this stability problem and managed to regulate the cavitation activity [5], [6].

This therapeutic technique still needs a monitoring system which would be essential to ensure the perfect and entire destruction of clots without damaging vessels. US monitoring techniques are currently used clinically for other treatments as for prostate cancer [7], computer assisted surgery [8] and HIFU. Last treatment can be monitored by mapping the rising tissue temperature and/or the cavitation activity. There is currently some clinically existing monitoring technique as MRI monitoring [9] by mapping the temperature rises and B-mode US [10] by turning off the therapy transducer between each acquisition. These techniques are not efficient in term of real time monitoring and spatial resolution. However some studies have already been made on the passive cavitation imaging [11], [12]. Gateau *et al.* worked on a technique combining passive and active detection of cavitation using a conventional ultrasonic array [13]. Passive detection was used to locate the bubble cloud and active detection to provide information on the temporal behavior over time of the first bubble induced. Coussios *et al.* are working on a passive acoustic mapping (PAM) technique used for spatial monitoring of HIFU therapy. They are currently working on the beamforming algorithm by combining time exposure acoustic (TEA), delay and sum (DAS) and robust capon beamforming (RCB) algorithms to improve resolution and reduce interference artifacts [14].

A passive US imaging system for monitoring in real time the US thrombolysis is under research and the goal is to locate spatially and in real time the cavitation activity. Time reversal (TR) method is often used to locate acoustic sources. It is used in our study to back-propagate the raw data acquired by a research US advanced open Platform (ULA-OP) [15] in a passive mode.

Thus, this work focuses on the integration of the monitoring system to the therapeutic set up and on the TR reconstruction method of the cavitation intensity map. In Part 2, the experimental setup and the post-processing method are described. Both the therapeutic and monitoring system are highlighted. The experimental results are exposed in Part 3. Finally, in Part 4, discussion about the results and further work is provided.

2 Method

2.1 Experimental setup

The general experimental setup consists in two separate systems. First, the therapeutic system, where a custom-manufactured transducer, a FPGA card (NI PXIe-7966R) and a needle-hydrophone (ONDA HNC-1500) are set up to create and regulate cavitation therapy [5]. The spherically-focused therapeutic transducer working at 1 MHz with a 100 mm active aperture is focalizing at 80 mm. The hydrophone and the FPGA card are used to create a feedback loop to regulate the cavitation intensity. A pulsed sinusoidal signal at frequency of 1 MHz is transmitted with 250 ms of pulse repetition and a duty cycle of 0.1. The signal is amplified by a power amplifier (69 dB, PRANA GN 1000) then sent to the therapeutic transducer. This system and the regulation loop were implemented by Desjouyet *al.* [5]. Regulated cavitation is used during this study so bubble clouds are much better observed and also to get the same results during the whole therapy. So the passive images are less related to the cavitation phenomena.

Second, a monitoring system is designed using the ULA-OP diagnostic open-platform with a linear probe of 192 elements (LA523, Esaote, Florence, Italy) working at 7 MHz central frequency with a -6 dB bandwidth of 4-12 MHz. During the acquisitions, a classical B-mode is used for the image reference of the setup and then, passive acquisitions are conducted to detect bubbles activity. The B-mode is an active imaging diagnostic mode using the whole 192 elements of the probe to form 192 beamformed lines with a frame rate of 20 images/s. Given the limitation of the ULA-OP system, 64 active elements are used for each RF lines. The passive mode is only using the central 64 active elements of the probe which are simultaneously acquiring the pre-beamformed signals. The US pulse transmission is turned off during passive acquisition so echoes only come from external sources as bubbles. The listening time depends on the depth of acquired images and can be modified using the open-platform.

The monitoring system is set with the therapeutic setup in the way that the diagnostic probe is placed at 90° relative to the US therapeutic beam. The probe is displayed to image the lateral resolution of the cavitation activity. In this experiment, a 10x10x10 cm³ agar gel cube (4%) is placed in the focus of the transducer. The full scheme of the experimental platform is presented in Fig. 1.

Using the FPGA system that control the therapeutic transducer, an external trigger signal has been created to synchronize the imaging system. Then, using appropriate delay, the passive recording can be conducted at any moment of the therapeutic ultrasound shot.

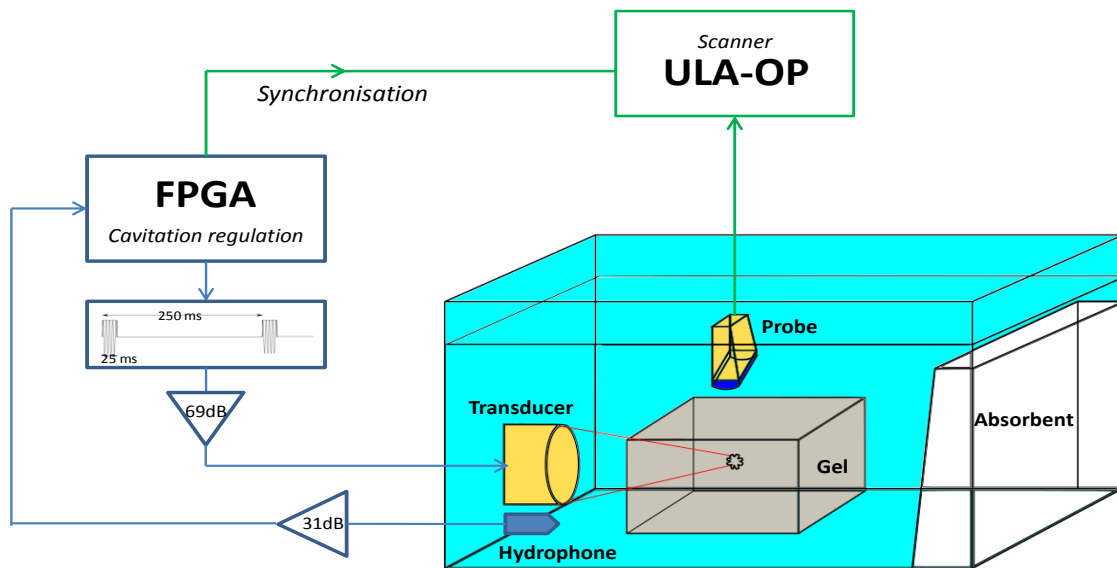


Fig.1 : experimental set-up of the full therapeutic and monitoring system. The FPGA card creates a pulsed sinusoidal signal which is amplified then sent to the therapeutic transducer. Thanks to the hydrophone a feedback cavitation regulation loop is created. An external trigger delivered by the FPGA synchronizes the passive acquisition on the ULA-OP scanner using a linear probe.

2.2 Post-processing

During different moment of cavitation exposure in the agar gel, the pre-beamformed signals from the passive probe were recorded and then post-processed using the software Matlab (Mathworks). The acquired raw data correspond to acoustic signal emitted by bubbles sources. These raw data are filtered by a band-pass filter to smooth the waves and are narrowed to choose the number of waves which correspond to the time of cavitation's exposure. TR method was applied using the toolbox "k-wave" developed for ultrasound simulation by Treeby *et al.* [16]. Parameters relative to the medium are set as the sound of speed distribution, the ambient density and the medium absorption factor. Each 64 elements of the probe are recording the pressure according to a same vector time. In the k-wave simulation, this vector time is reversed and then the pressure raw data are emitted to focus the wave back to the source. The vector time of the input signal is chosen long enough such that the back propagated wave have enough time to go back to the acoustic source. The wave's propagation is simulated by solving the first order wave's equations:

$$(1) \rightarrow \frac{\partial u}{\partial t} = -\frac{1}{\rho_0} \nabla p$$

$$(2) \rightarrow \frac{\partial p}{\partial t} = -\rho_0 \nabla \cdot u$$

$$(3) \rightarrow p = c_0^2 \rho$$

These equations are based on the conservation of momentum (1), conservation of mass (2) and the pressure-density relation (3). u is the acoustic particle velocity, p is the acoustic pressure, ρ is the acoustic density, ρ_0 is the ambient density and c_0 is the isentropic sound speed.

The maximum of intensity is then computed and the cavitation intensity map is found.

3 Results

In this study, only the beginning and the end of the 25 ms cavitation pulse were recorded using the external trigger of the FPGA. The passive images were computed from raw data received by the 64 channels of the passive probe and shown in Fig.2. The black sections correspond to the moment when the therapeutic transducer is turned off. The white lines correspond to acoustic signal diffused by bubbles. A radio frequency (RF) signal recorded by the 32th element of the probe is shown in Fig.2.c matching the 32th line of the passive image Fig.2.b. The end of the cavitation activity occurring at 27 μ s can be seen in the RF signal. The Fourier transform of this RF signal is illustrated in Fig.2.d. Peaks are observed at specific frequency corresponding to harmonics from 1 to 8 MHz. These harmonics stress the non-inertial cavitation activity. Broadband noise is also noticed which is for the most part created by inertial cavitation.

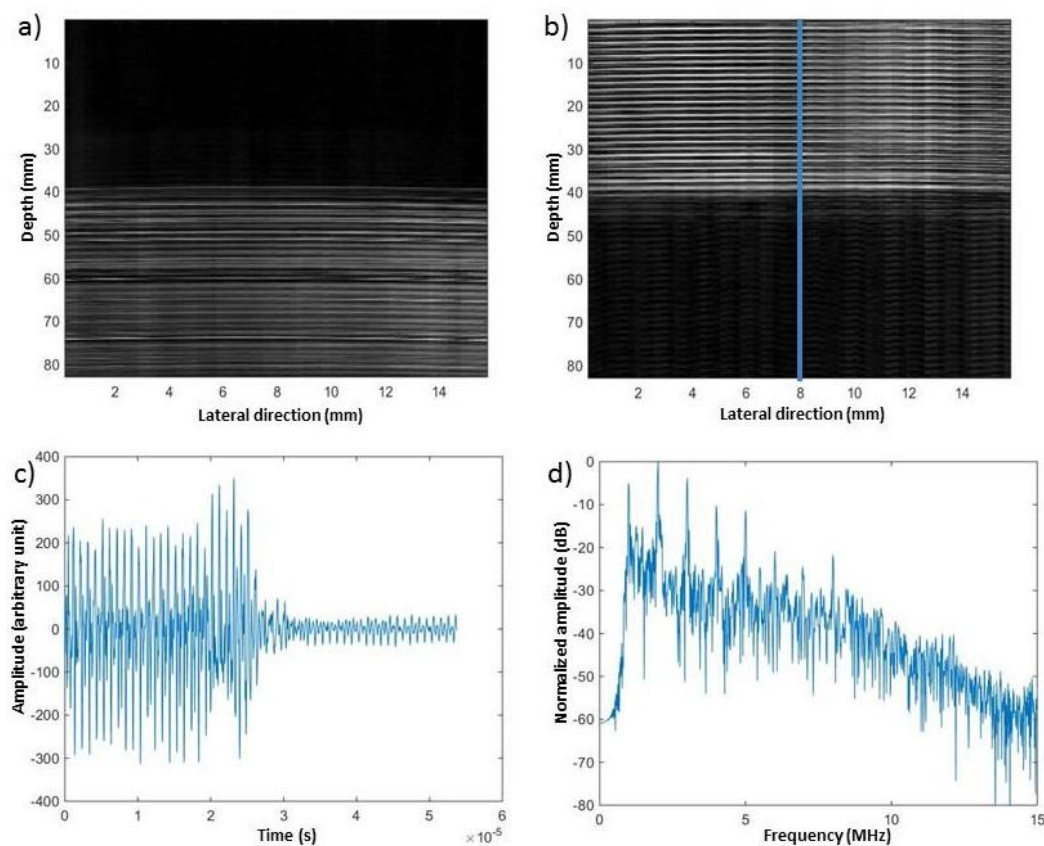


Fig.2 : a) passive image of cavitation during the beginning of the therapeutic pulse, b) passive image cavitation during the end of therapeutic pulse, c) RF signal recorded for element 32 corresponding to the 32th line of the image b, c) frequency spectrum of RF signal of figure c

The raw data of the image Fig.2.b were filtered with a 5.5-6.5MHz band-pass filter and were narrowed to 6 acoustic waves corresponding to 10 μ s using the TR method on these acoustic waves, the cavitation intensity map is obtained and illustrated in Fig.3.a. The reference B-mode image is also acquired in

Fig.3.b. The same probe aperture, 192 elements corresponding to 47 mm aperture, was used for both images. In the cavitation intensity map, the cavitation spot is noticed at 60mm deep with 20mm length and 1mm wide. In the B-mode image, the cavitation spot is tracked by searching hyper-echoes structures which correspond to bubbles observed at 70mm deep matching the theoretical focused therapeutic beam. Taking into account the possible cavitation damage to the diagnostic probe, it is inserted as close as possible to the bubble cloud. This problem could be solved by integrating the probe coaxially to the therapeutic transducer.

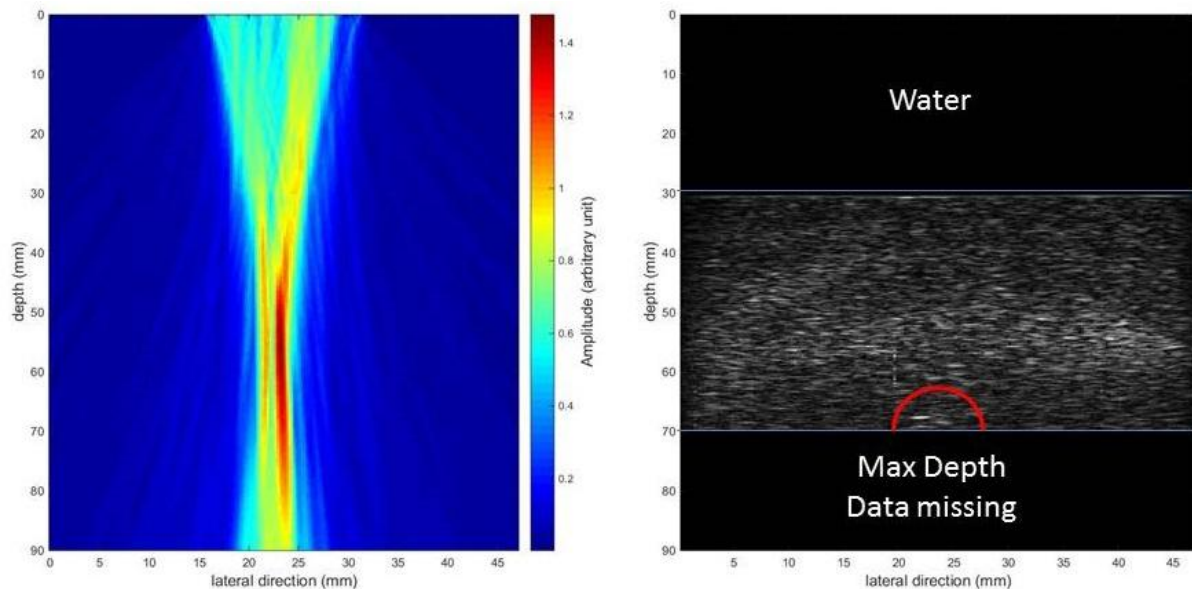


Fig. 3 : a) cavitation intensity map, b) B-mode reference image.

4 Discussion and Conclusion

The lateral localization of the cavitation spot observed in the cavitation intensity map and the B-mode image are highly similar. However the depth resolution of the cavitation spot needs improvements. In Fig.2.d the harmonics 5 to 8 MHz belong to the probe's bandwidth (5-9 MHz) so their observation is normal. The remaining harmonics (1 to 4 MHz) are observed because the energy delivered is so strong that they are still present in the recorded signal. The use of higher frequency during the TR led to better lateral resolution. Time between the creation of a bubble and his collapse was not considered during processing and was neglected. The acoustic wave signals are sharper in the end (Fig.2.b) than at the beginning of the therapeutic pulse (Fig.2.a). This can be explained by the fact that in the beginning of the therapeutic pulse the cavitation regulation is less efficient than in the end where it have reached the best outcome. Stack of acoustic waves were processed by TR. Instead of sending the entire stack, they can be separated in individual acoustic waves, back-propagated and finally the intensity averaged. Inertial and non-inertial cavitation activity could be separated so two specific maps could be computed. Work still need to be done on the precision and resolution of the intensity map. In further studies the probe could be integrated coaxially to the therapeutic transducer so the axial resolution of the therapeutic beam is processed. The utilization of nonconsecutive element in passive receive will also be investigated. Recalling the goal to get a real-time monitoring system, the signal processing stage should be fast enough. TR method is too much time consuming and so is not the best way to resolve this real-time problem. However it is a first step in our study to calibrate the cavitation focal region. Other passive detection technique will be the focus of future work.

5 Acknowledgment

This work was supported by the Labex CeLyA (ANR-10-LABX-0060) of Université de Lyon within the program “Investissements d’Avenir” (ANR-11-IDEX-0007) and by the French national research agency project “ULysSE” (ANR-11-JSV5-0008).

6 References

- [1] G. Harvey, A. Gachagan, and T. Mutasa, “Review of high-power ultrasound-industrial applications and measurement methods,” *IEEE Trans. Ultrason. Ferroelectr. Freq. Control*, vol. 61, no. 3, pp. 481–495, Mar. 2014.
- [2] J. E. Lingeman, J. A. McAteer, E. Gnessin, and A. P. Evan, “Shock wave lithotripsy: advances in technology and technique,” *Nat. Rev. Urol.*, vol. 6, no. 12, pp. 660–670, Dec. 2009.
- [3] C. D. Adrien Poizat, “Regulation of cavitation activity in pulsed sonication with a real-time feedback loop system,” 2013.
- [4] H.-D. Liang, J. Tang, and M. Halliwell, “Sonoporation, drug delivery, and gene therapy,” *Proc. Inst. Mech. Eng. [H]*, vol. 224, no. 2, pp. 343–361, Feb. 2010.
- [5] C. Desjoux, A. Poizat, B. Gilles, C. Inserra, and J.-C. Bera, “Control of inertial acoustic cavitation in pulsed sonication using a real-time feedback loop system,” *J. Acoust. Soc. Am.*, vol. 134, no. 2, pp. 1640–1646, Aug. 2013.
- [6] A. Poizat, D. Cyril, I. C. G. Bruno, and B. Jean-christophe, “Régulation temporelle de l’activité de cavitation ultrasonore en régime pulsé,” *CFA 2014*, pp. 1173–1179.
- [7] L. Mearini and M. Porena, “Transrectal high-intensity focused ultrasound for the treatment of prostate cancer: Past, present, and future,” *Indian J. Urol. IJU J. Urol. Soc. India*, vol. 26, no. 1, pp. 4–11, 2010.
- [8] T. K. Chen, P. Abolmaesumi, D. R. Pichora, and R. E. Ellis, “A system for ultrasound-guided computer-assisted orthopaedic surgery,” *Comput. Aided Surg. Off. J. Int. Soc. Comput. Aided Surg.*, vol. 10, no. 5–6, pp. 281–292, Nov. 2005.
- [9] C. Damianou, M. Pavlou, O. Velez, K. Kyriakou, and M. Trimikliniotis, “High intensity focused ultrasound ablation of kidney guided by MRI,” *Ultrasound Med. Biol.*, vol. 30, no. 3, pp. 397–404, Mar. 2004.
- [10] S. Vaezy, X. Shi, R. W. Martin, E. Chi, P. I. Nelson, M. R. Bailey, and L. A. Crum, “Real-time visualization of high-intensity focused ultrasound treatment using ultrasound imaging,” *Ultrasound Med. Biol.*, vol. 27, no. 1, pp. 33–42, Jan. 2001.
- [11] V. A. Salgaonkar, S. Datta, C. K. Holland, and T. D. Mast, “Passive cavitation imaging with ultrasound arrays,” *J. Acoust. Soc. Am.*, vol. 126, no. 6, pp. 3071–3083, Dec. 2009.
- [12] K. J. Haworth, T. D. Mast, K. Radhakrishnan, M. T. Burgess, J. A. Kopechek, S.-L. Huang, D. D. McPherson, and C. K. Holland, “Passive imaging with pulsed ultrasound insonations,” *J. Acoust. Soc. Am.*, vol. 132, no. 1, pp. 544–553, Jul. 2012.
- [13] J. Gateau, J.-F. Aubry, M. Pernot, M. Fink, and M. Tanter, “Combined passive detection and ultrafast active imaging of cavitation events induced by short pulses of high-intensity ultrasound,” *IEEE Trans. Ultrason. Ferroelectr. Freq. Control*, vol. 58, no. 3, pp. 517–532, Mar. 2011.
- [14] C. Coviello, R. Kozick, J. Choi, M. Gyöngy, C. Jensen, P. P. Smith, and C.-C. Coussios, “Passive acoustic mapping utilizing optimal beamforming in ultrasound therapy monitoring,” *J. Acoust. Soc. Am.*, vol. 137, no. 5, pp. 2573–2585, May 2015.
- [15] P. Tortoli, L. Bassi, E. Boni, A. Dallai, F. Guidi, and S. Ricci, “ULA-OP: an advanced open platform for ultrasound research,” *IEEE Trans. Ultrason. Ferroelectr. Freq. Control*, vol. 56, no. 10, pp. 2207–2216, Oct. 2009.
- [16] B. E. Treeby and B. T. Cox, “k-Wave: MATLAB toolbox for the simulation and reconstruction of photoacoustic wave fields,” *J. Biomed. Opt.*, vol. 15, no. 2, pp. 021314–021314–12, 2010.